which clearly contradicts the initial assumption. Thus, the right-hand side of the matrix equation must have rank equal to $P - Q$. Since the module equations themselves have full rank, by hypothesis, that is

$$\begin{bmatrix} G \\ F \\ A \end{bmatrix} \text{ has rank } N$$

it follows that the matrix of solutions V must have rank $P - Q$. Thus, the solutions generated from the $z^{(J)}$ must be linearly independent, and the proposition is verified.

Manuscript received December 21, 1977; revision received August 18, and accepted September 6, 1978.

Use of a Finite-Stage Transport Concept for Analyzing Residence Time Distributions of Continuous Processes

REED S. C. ROGERS

and

ROBIN P. GARDNER

Departments of Nuclear and Chemical Engineering
North Carolina State University
Raleigh, North Carolina 27650

This study is concerned with the derivation and application of the finite-stage transport concept for modeling residence time distributions (RTD's) originally proposed by Adler and Hovorka (1961). This six-parameter model is shown to be more versatile and accurate than the common two-parameter tanks-in-series or axial dispersion models. Radioactive tracer results are given for a number of particulate unit processes with special emphasis on wet-discharge ball mills.

SCOPE

The residence time distribution (RTD) concept is becoming more and more important to chemical engineers in the modeling of continuous, first-order processes by the segregated flow approach (Himmelblau and Bischoff, 1968; Levenspiel, 1962). It is very advantageous to have analytical functions for the RTD's encountered as evidenced by interest in the simple two-parameter tanks-in-series and axial dispersion models. These simple models often do not offer sufficient versatility or accuracy. Therefore, the present paper reexamines a previously proposed six-parameter, finite-stage transport concept for increased versatility and accuracy.

To accomplish this objective, a complete derivation of the model is included, along with an accurate and efficient parameter estimation method for it. In addition, the model is incorporated into the segregated flow concept to model a general first-order process. Finally, radioactive tracer results for a number of particulate unit processes with emphasis on wet-discharge ball mills are given which indicate the increased versatility and accuracy of this model over the simple two-parameter models.

CONCLUSIONS AND SIGNIFICANCE

In this study, the finite-stage transport concept of Adler and Hovorka (1961) is investigated as a general transfer function for industrial process analysis. Application of the model is demonstrated experimentally on several continuous particulate mineral processes. The study indicates that the parameter estimation method proposed can provide a high degree of accuracy for fitting the finite-stage model to actual data and that it is possible to obtain explicit, closed-form analytical solutions to a wide class of steady state first-order processes by the use of the segregated flow concept with this model. Extensions of the model and experimental methods that are often necessary or desirable when using radioactive tracers have also been derived and demonstrated.

The finite-stage transport concept has the advantages over the simpler tanks-in-series and axial dispersion models of greater versatility and improved accuracy. It provides these advantages while still yielding analytical models for first-order process phenomena when the segregated flow concept is used. The axial dispersion model does not

Correspondence concerning this paper should be addressed to Robin P. Gardner.

have this feature. These advantages are realized at the expense of having to employ nonlinear search methods for parameter estimation and of having a relatively complex analytical model. Each potential user must decide if these advantages outweigh the disadvantages for his particular application.

The parameter estimation method described here has been implemented by the development of a computer program. This program has been written and documented as a subroutine in FORTRAN called NCSRTD. A listing of the FORTRAN statements is available from the authors.

The major use of this model by the authors has been an extensive program of study to characterize the residence time distribution (RTD's) of industrial ball mills of various types and under various operating conditions. From the data obtained so far, it appears that five of the six finite-stage model parameters are constant for RTD's measured on a wide range of industrial, wet ball mills of the overflow time. This surprising result, if found to be generally true, would allow a very large reduction in the computational effort required for parameter estimations.

This model should prove generally useful to researchers interested in developing models of the segregated flow type for continuous, first-order processes. It is versatile enough to provide excellent accuracy while retaining the feature of yielding analytical solutions.

The authors have conducted (Gardner, Rogers, and Verghese, 1977) and are aware of a number of other experiments in which short-lived radioactive tracers were used to measure the residence time distributions (RTD's) of various continuous, particulate mineral processes. In general, it has been found that simple transport concepts, such as the tanks-in-series and axial dispersion models, are not sufficiently accurate. As a result, the present study was undertaken to investigate the finite-stage transport model proposed by Adler and Hovorka (1961). In addition to increased versatility and accuracy, this model also has the advantages that it reduces to the tanks-in-series model and it yields analytical models for common first-order processes when used with the segregated flow concept.

Included here is a complete derivation of the finite-stage transport model of Adler and Hovorka (1961) and an accurate and efficient parameter estimation method for it. This model is applied to RTD data obtained for a screw classifier and for several open-circuit, full scale ball mills. Also developed here is a steady state model which incorporates this transport concept for a general, first-order continuous process.

THE BASIC MODEL

The basic stage of the finite-stage transport concept as seen in Figure 1 consists of two interconnected perfectly mixed tanks and one plug flow tank. The lower perfectly mixed tank approximates dead or stagnant flow regions, while the upper perfectly mixed tank approximates live or active flow regions. The connecting flow between the two allows an interchange between the live and dead flow regions as one would expect in a real flow system. The plug flow tank represents a simple time delay. This basic stage of the model may repeat itself an integer number of times.

The tracer impulse response for n stages of this model is given by

$$C_n^*(t) = C_n(t - F_c\tau)H(t - F_c\tau) \qquad (1)$$

where $H(t - F_c\tau)$ is the unit (positive) step function, and $C_n(t)$ is given by

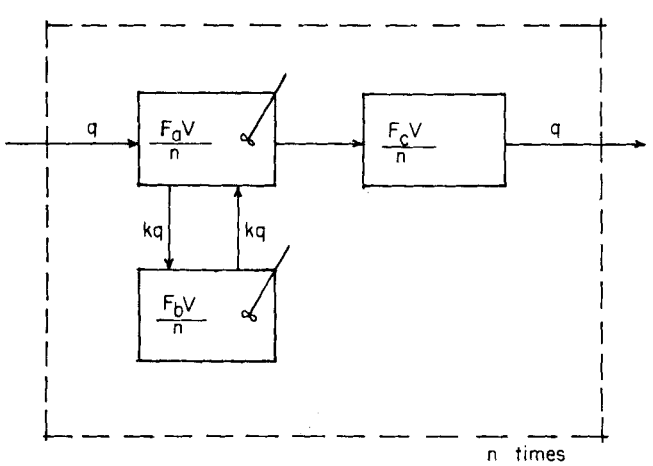

Fig. 1. Schematic diagram of the basic stage of the finite-stage transport concept.

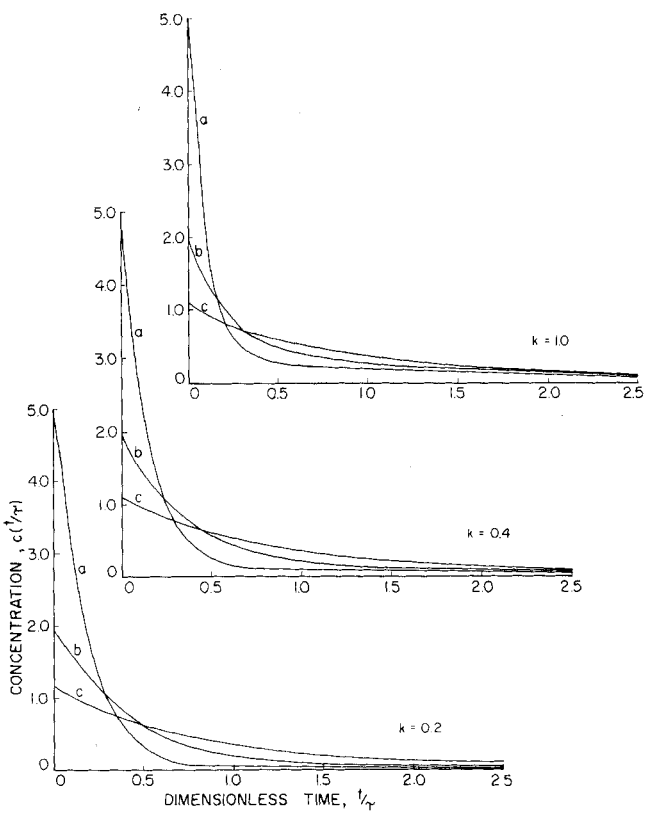

Fig. 2. Typical residence time distributions obtained from finite-stage transport model with $n = 1$, $F_a = 0.2$, (curve b), and $F_a = 0.9$ (curve c).

$$C_n(t) = (C^oV/q)\left(\frac{n}{F_a\tau}\right)^n \sum_{j=1}^{2}\sum_{l=1}^{n} \frac{\phi_l(m_j)t^{n-l}e^{m_j t}}{(n-l)!(l-1)!} \tag{2}$$

The m_j and $\phi_l(m_j)$ are algebraic expressions involving the parameters of the model; these and a complete derivation of the model are given in Appendix A. The residence time distribution is obtained directly from

$$\phi(t) = C_n^*(t) \Big/ \int_o^\infty C_n^*(t)dt \tag{3}$$

It can be shown that the zeroth and first moments of $\phi(t)$ are properly unity and the average residence time τ, respectively. The variance for this distribution is given by

$$\sigma^2 = (\tau^2/n)[(F_a + F_b)^2 + 2F_b^2/k] \tag{4}$$

TYPICAL MODEL RESPONSES

The versatility of the finite-stage transport model is illustrated in Figures 2, 3, and 4. Concentration is plotted vs. dimensionless time t/τ for various model parameter values. Since the plug flow tanks represent a simple time delay, the parameter F_c is taken to be zero in all of the examples since the effect of this parameter is obvious. The number of basic stages n takes the values 1, 3, and 6; the fraction that is live flow region F_a is taken to be 0.2, 0.5, and 0.9, and the fraction of cross flow k is taken to be 0.2, 0.4, and 1.0.

ESTIMATION OF MODEL PARAMETERS

The method presented here for estimating model parameters was developed specifically for analyzing RTD data obtained using short-lived radioactive isotopes as the tracer. However, the method can be used for non-radioactive tracers by making the term unity which takes into account radioactive decay of the tracer.

The response of a radiation detection system to an impulse injection of radioactive tracer is obtained from

$$y(t) = YC_n^*(t)f(t) + r_B \tag{5}$$

where the function $f(t)$ takes into account the radioactive decay of the tracer. The total amount of tracer injected is obtained by applying the principle of continuity:

$$Q = q\int_o^\infty C_n^*(t)dt \tag{6}$$

Substitution of $C_n^*(t)$ obtained from Equation (3) and $\int_o^\infty C_n^*(t)dt$ obtained from Equation (6) into Equation (5) gives

$$y(t) = A\phi(t)f(t) + r_B \tag{7}$$

where

$$A = YQ/q \tag{8}$$

Equation (7) is the working equation used to model the detector response with the finite-stage transport concept.

All of the parameters needed in Equation (7), with the exception of $f(t)$, can be determined directly by nonlinear least-squares analysis of the differences between the detector response and the model values predicted by the parameters chosen. However, this would be very inefficient and would require an inordinant amount of computer time. In general, one should attempt to reduce the number of parameters to be determined by a nonlinear method, since each additional parameter requires a correspondingly large amount of computer time. In the present case, a number of parameters can be eliminated.

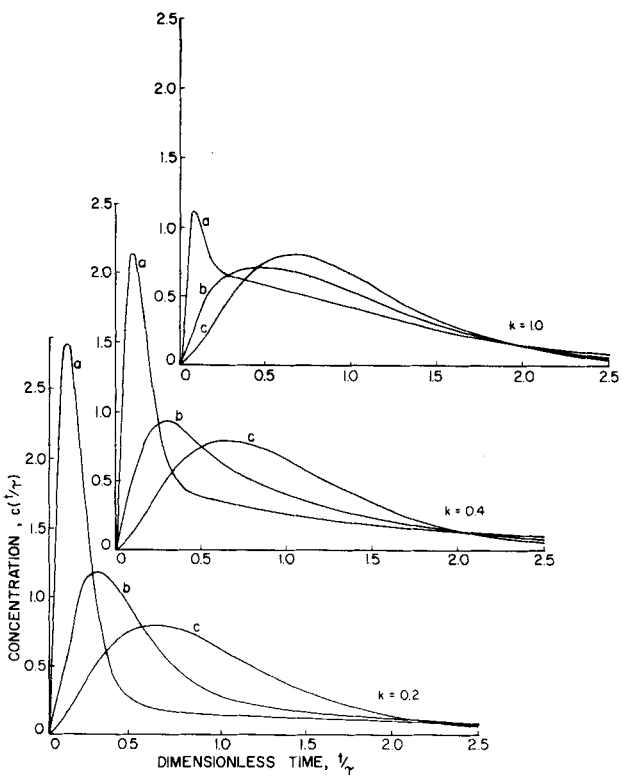

Fig. 3. Typical residence time distributions obtained from the finite-stage transport model with $n = 3$, $F_a = 0.2$ (curve a), $F_a = 0.5$ (curve b), and $F_a = 0.9$ (curve c).

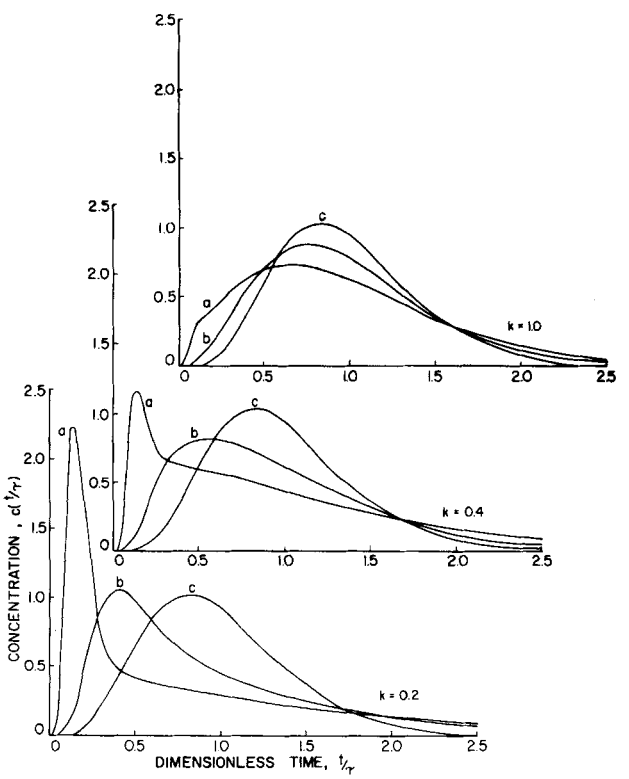

Fig. 4. Typical residence time distributions obtained from the finite-stage transport model with $n = 6$, $F_a = 0.2$ (curve a), $F_a = 0.5$ (curve B), and $F_a = 0.9$ (curve c).

TABLE 1. AVERAGES AND RELATIVE STANDARD DERIVATIONS OF MODEL PARAMETERS OBTAINED BY THE PARAMETER ESTIMATION METHOD FOR SIMULATED DETECTOR RESPONSE DATA

Parameter	True value	Average value	Relative standard deviation (%)
n	3	3	—
F_a	0.5	0.5005	0.18
F_b	0.5	—	—
F_c	0.0	0.0000	—
k	0.2	0.1990	0.42
A	128 000	127 937	0.35
r_B	200	209	5.33
τ	15.0	15.0	1.95

First of all, the function $f(t)$ is best determined experimentally by setting aside a small sample of the tracer to be used. This sample is counted at intervals over the time period of tracer use with the same radiation detector system and under the same conditions as for the actual tracer experiment. The net counting rate at any time divided by the initial net counting rate gives the function $f(t)$ directly. If a more quantitative and elaborate method is desired, particularly for those cases where more than one radioisotope is involved, one may fit the data by least squares to the model

$$f(t) = \sum_{k=1}^{m} a_k \exp(-\lambda_k t) \tag{9}$$

where the a_k and, if desired, also the λ_k are model constants that are determined by the least-squares analysis. In some cases, the λ_k, which are the decay constants for the various radioisotopes, will be known and need not be determined by the least-squares analysis.

The parameter F_b is obtained for given values of F_a and F_c from the identity

$$F_b = 1 - F_a - F_c \tag{10}$$

The parameters A and r_B are the linear parameters in Equation (7) and can therefore be obtained by an explicit, linear, least-squares method when values of the other model parameters are specified. The integer parameter n is determined by fixing it at a constant given value until optimum values of the other parameters have been obtained. Then n is incremented, and optimum values of the other parameters are again obtained. The optimum value of n is taken as that which gives the best overall fit of the model equation to the actual detector response data. Finally, in cases where the feed rate and holdup of a process are known, τ may be obtained from the identity relationship $\tau = V/q$; however, in the present discussion, it is assumed that τ is unknown. This leaves the parameter F_a, k, τ, and F_c to be determined directly by a nonlinear method for each search value of n. The nonlinear method used here is a modification of the method given by Bevington (1969) in a computer program called CURFIT. The program CURFIT minimizes the reduced chi-squared value by a combined linear approximation and gradient search method.

Hence, at the end of each parameter search using the chosen value for n, the parameter F_b is calculated from the new values of F_a and F_c. The parameters A and r_B are determined by a linear least-squares method, and the reduced chi-squared value is calculated and compared to the value calculated at the end of the previous iteration. When a minimum reduced chi-squared value has been obtained for the value of n chosen, n is incremented and the analysis repeated. The optimum values for all of the parameters are obtained from the trial value of n which gives the overall minimum reduced chi-squared value.

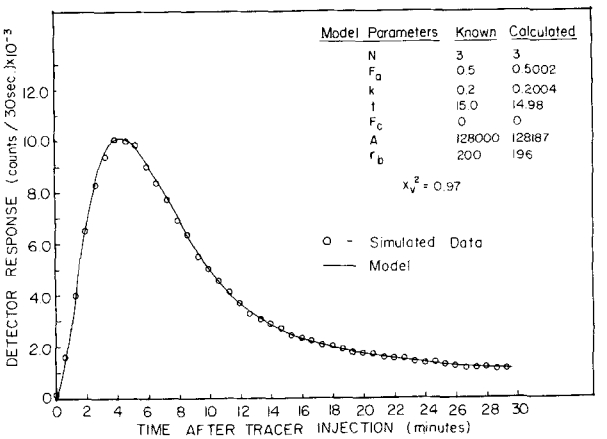

Fig. 5. Simulated detector response data fitted to the finite-stage transport model.

This parameter estimation method calls for initial estimates for the parameters F_a, k, τ, F_c, and n. While accurate results may be obtained from initial estimates which differ from the final values by as much as 100%, a substantial savings in computer time is made possible by using the following techniques to calculate the initial estimates.

First, if the maximum detector response occurs at time zero, n is taken to be one; otherwise, the initial value is taken as two. An initial estimate for τ can be obtained from the actual data from

$$\tau \cong \sum_{i=1}^{p} t_i(y_i - r_B^*)f(-t_i)\Delta t_i \Big/ \sum_{i=1}^{p} (y_i - r_B^*)f(-t_i)\Delta t_i \tag{11}$$

The parameter F_c may be estimated by

$$F_c = \tau_c/\tau \tag{12}$$

Next, F_a and F_b are estimated by

$$F_a = F_b = (1 - F_c)/2 \tag{13}$$

and the estimate for k is arbitrarily taken to be 0.2. Estimates for A and r_B are not required, since they are calculated by the linear least-squares method using the initial estimates for all of the other parameters. When optimum values of these parameters have been obtained, n is incremented by one and the analysis repeated until the overall minimum chi-squared value is obtained.

The sensitivity and accuracy of the method was investigated by simulating a detector response curve that one might expect to obtain when using a radioactive tracer. Counting rates vs. time after tracer injection were calculated using a known set of parameter values in Equation (7) such that the maximum counting rate times the counting interval in which it was obtained, $[y_i\Delta t_i]_{max}$, did not exceed 10 000 counts. It was then assumed that the counting rate data were Poisson distributed as would be the case for real counting rate data, and simulated real values were generated by a random number process. The new values were chosen randomly from a normal distribution with mean and variance of $y_i\Delta t_i$ as would be proper for a Poisson distribution. The

parameter estimation method was applied to several of these statistically distributed detector response curves and was found to be quite accurate. The known parameter values and those that were backcalculated are listed in Table 1. An example of the statistically distributed data and the model fit to the data can be seen in Figure 5.

APPLICATIONS TO SELECTED PARTICULATE PROCESSES

In a series of short-lived radioactive tracer tests, the RTD's of a pilot plant scale screw classifier and several full scale industrial, open-circuit ball mills have been measured. In these cases, analysis of the data required extension or modification of the finite-stage model to account for necessary anomalies in the experimental arrangement. Since these anomalies are likely to be encountered when radioactive tracers are used, a brief description of the experimental methods and necessary extensions of the model are included in the following discussion. A more complete description of the experimental methods is found in the paper by Gardner, Rogers, and Verghese (1977).

In all of these tests, the tracer was a sample of the feed to the process which has been irradiated in a nuclear reactor. The irradiated sample was injected as an impulse into the process feed while the process was in normal steady state operation. For the wet processes described in the following, RTD's were obtained by directing the process product to a constant volume, constantly stirred sump in which a radiation detector was immersed. With this counting sump method, the counting rate of the detector is proportional to the amount of radioactive tracer in the sump; the RTD is thus measured by continuous monitoring of counting rate in the sump vs. time after tracer injection.

It should be noted that the use of the counting sump method necessitates knowing the RTD of the sump itself,* since the data obtained will be the RTD of the combined process and sump. It is, therefore, a convolution of the process and sump RTD's, stated mathematically as

$$\phi_T(t) = \int_o^t \phi(t')\phi_s(t - t')dt' \qquad (14)$$

where $\phi(t)$, $\phi_s(t)$, and $\phi_T(t)$ are the RTD's of the process, the sump, and the process and sump together, respectively. Assuming that $\phi(t)$ is the finite-stage transport model, measuring and modeling $\phi_s(t)$ allows the derivation of an analytical expression for $\phi_T(t)$. The unknown parameters of $\phi(t)$ are then backcalculated with the parameter estimation method by fitting the $y(t)$ obtained from Equation (7) with $\phi(t)$ replaced by $\phi_T(t)$ to the counting rate data obtained in the sump. Models for $\phi_T(t)$, where $\phi_s(t)$ is assumed to be a single, perfectly mixed tank and two perfectly mixed tanks-in-parallel are found in Appendix B [Equations (B3) and (B8), respectively].

The pilot plant screw classifier on which an RTD test was conducted was used to deslime a slurry of alaskite ore and water. The solids feed rate was about 21.4 g/s. The counting sump used in this experiment was a well-mixed 2 gal cylindrical tank whose solids holdup was determined to be about 9.08 kg. The sump RTD was modeled as a single perfectly mixed tank with an average residence time of 7.1 min; thus, RTD data

* Actually, the RTD of the sump is not exactly what is required. One requires the pseudo residence time distribution that is obtained by injecting a tracer at the sump entrance and monitoring the concentration in the sump with an immersed detector. Since this is what is obtained experimentally and used in all subsequent calculations, it is simply referred to as the sump residence time distribution throughout this paper.

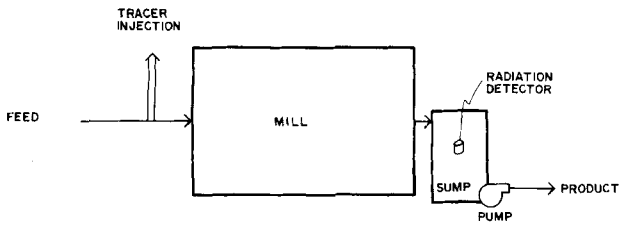

Fig. 6. Actual and fitted residence time distributions obtained for alaskite ore being dewatered in a pilot plant scale screw classifier.

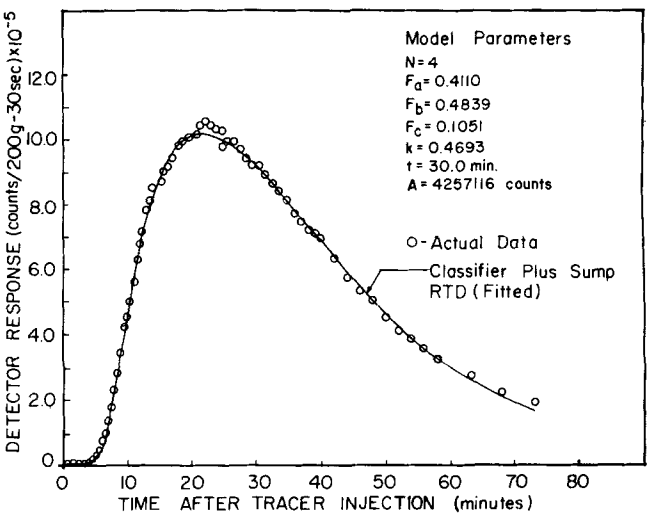

Fig. 7. Schematic diagram of the experimental method used to measure the residence distribution of a large scale, industrial, wet, ball mills.

for the classifier plus sump was fitted to Equation (7), where $\phi(t)$ is as the modified transport model of Equation (B3) of Appendix B. Figure 6 is a plot of the actual and fitted data as well as the finite-stage model RTD determined from the backcalculated parameters.

Several measurements were made on a 1.83 m × 2.74 m industrial ball mill operating in the wet mode. A schematic of the mill system is seen in Figure 7. The mill was operated at 60% solids. The grinding media was 5.08 cm diameter steel balls, and sand was the material being ground. The pumping sump in which radiation detectors were submerged had a volume of about 0.605 m^3 and was operated at 30 to 50% solids. RTD measurements were made for solids feed rates of 7.6, 8.6, 9.6, and 10.6 kg/s. Before each test was conducted, the RTD of the pumping sump was measured by injecting a small amount of irradiated sand into the sump with the mill product and measuring the counting rate vs. time after tracer injection. The sump RTD's were modeled as two tanks in parallel; Figure 8 is a typical plot of actual data and fitted values from the two tanks in parallel model. Data for the mill plus sump RTD's were fitted to the transport model given by Equation (B8) of Appendix B. Figures 9, 10, 11, and 12 are plots of the actual and fitted data as well as the finite-stage model RTD determined from the backcalculated parameters for the respective feed rates.

The most recent tests were conducted on two full scale, industrial, ball mills. Both of these mills were used for the wet grinding of phosphate ore. The smaller mill, approximately 3.81 m in diameter and 5.18 m long, was operated at feed rates of 17.7, 21.4, and 25.2 kg/s. The larger mill, 4.57 m in diameter and 9.30 m long, was operated at 40.4, 44.1, and 51.7 kg/s. In both mills, the slurry was 67% solids, and 5.08 diam steel balls were the grinding media. As with the earlier work, tests

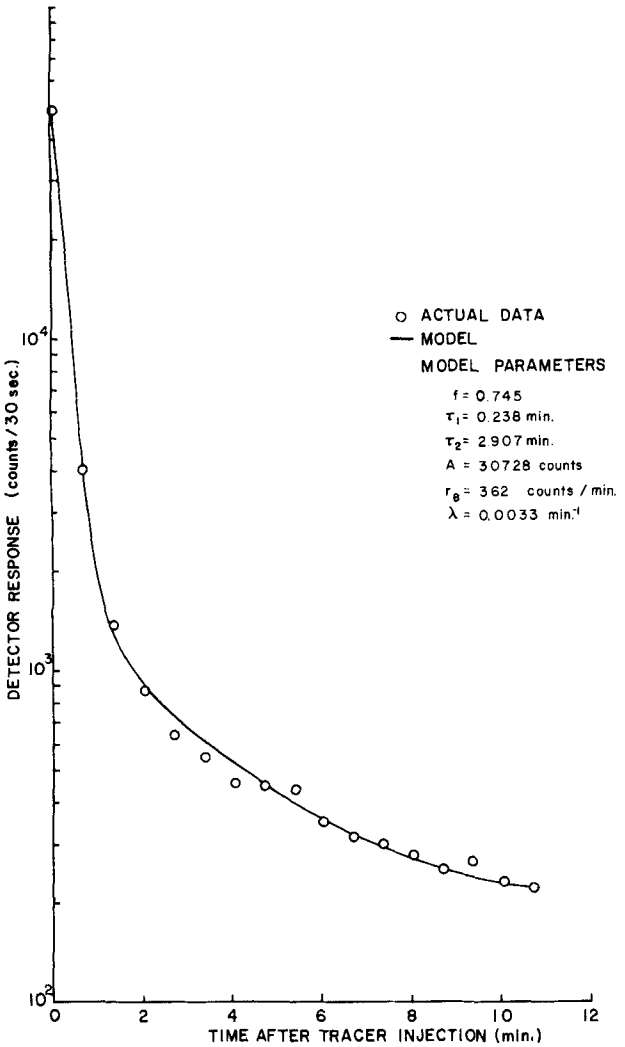

Fig. 8. Actual and fitted detector response data obtained for the pumping sump of the 1.83 m × 2.74 m industrial, wet, ball mill at a mill feed rate of 7.6 kg/s.

were made to obtain the sump RTD's at the various feed rates for both mills. The sump RTD's were modeled as single, perfectly mixed tanks. Figures 13 and 14 are examples of the data obtained from these sump tests* plotted along with model predictions. Data for the mill plus sump RTD's were fitted to the transport model given by Equation (B3) of Appendix B. Figures 15 through 20 are plots of the actual and fitted mill plus sump data as well as the mill model RTD determined from the backcalculated finite-stage parameters for the respective mills and feed rates tested.

DISCUSSION OF RESULTS

Experimental results have been presented for RTD measurements made on a screw classifier and several large scale, open-circuit, wet, ball mills. The RTD data have been analyzed according to the finite-stage model using the described parameter estimation method. While it is apparent that the finite-stage model accurately reproduces the data, it seems appropriate to point out

* A simple time delay was observed between tracer injection into the sump and initial detector response. This plug flow response was treated by defining τ_p as the duration of the time delay. The appropriate model for the sump is then given by

$$\phi_s(t) = \exp\left[-(t-\tau_p)/\tau_s\right] H(t-\tau_p)/\tau_s$$

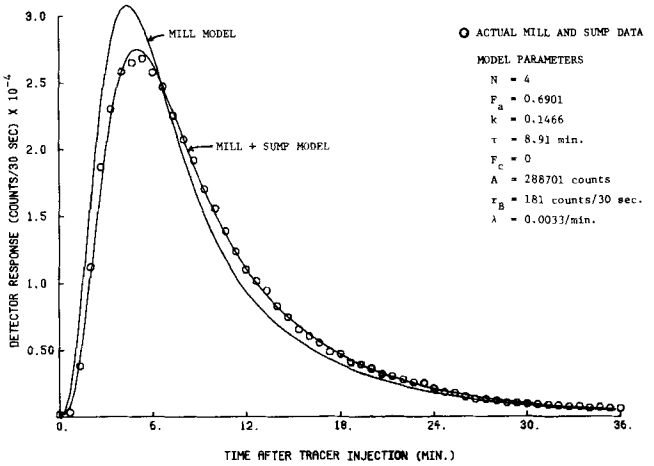

Fig. 9. Actual and fitted detector response data obtained for the 1.83 m × 2.74 m industrial, wet, ball mill at a mill feed rate of 7.6 kg/s.

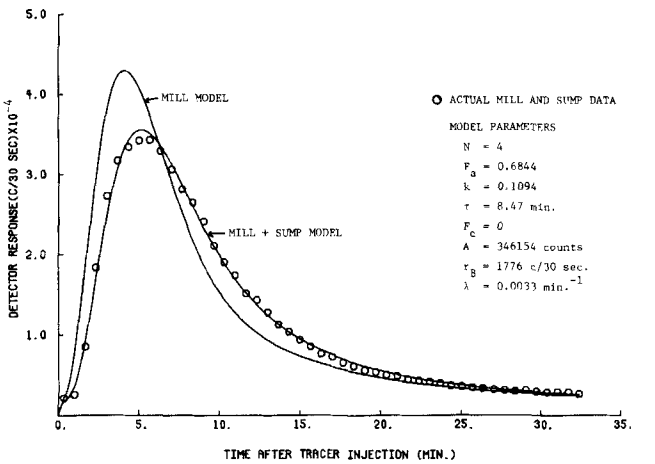

Fig. 10. Actual and fitted detector response data obtained for the 1.83 m × 2.74 m industrial, wet, ball mill at a mill feed rate of 8.6 kg/s.

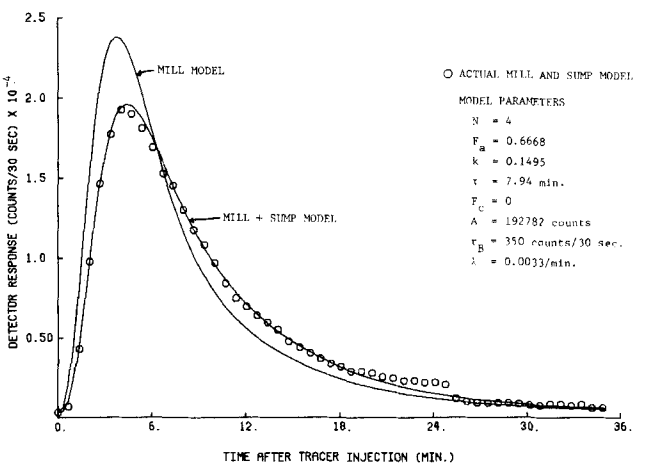

Fig. 11. Actual and fitted detector response data obtained for the 1.83 m × 2.74 m industrial, wet, ball mill at a mill feed rate of 9.6 kg/s.

the advantages of using this model over simpler transport models in present popular use.

First of all, the dimensionless* RTD of the classifier is very different than that of the ball mills. This would be observed regardless of the RTD model considered;

* $\phi(t/\tau)$ vs. t/τ.

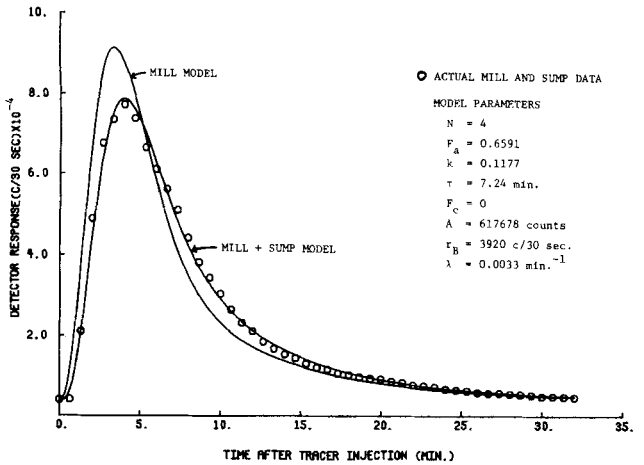

Fig. 12. Actual and fitted detector response data obtained for the 1.83 m × 2.74 m industrial, wet, ball mill at a mill feed rate of 10.6 kg/s.

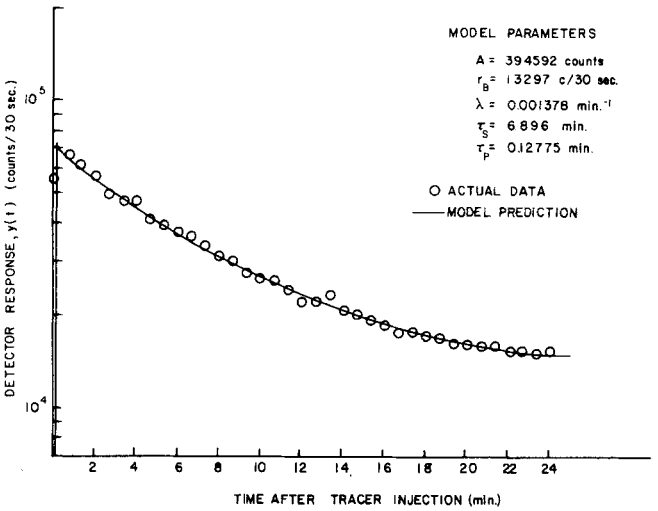

Fig. 13. Actual and fitted detector response data obtained for the pumping sump of the 3.81 m × 5.18 m industrial wet, ball mill at a mill feed rate of 25.2 kg/s.

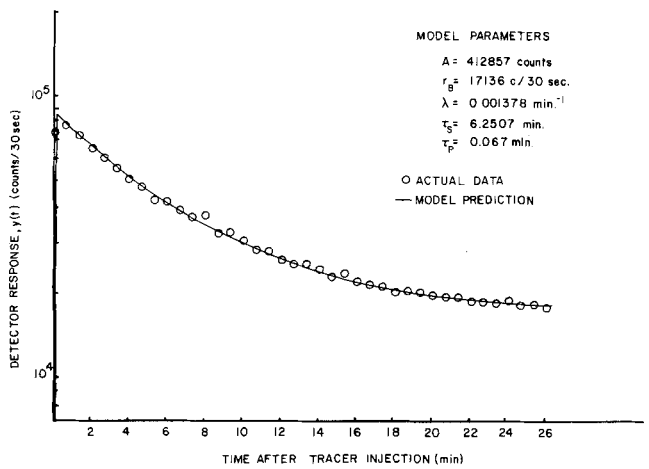

Fig. 14. Actual and fitted detector response data obtained for the pumping sump of the 4.57 m × 9.30 m industrial, wet, ball mill at a mill feed rate of 40.4 kg/s.

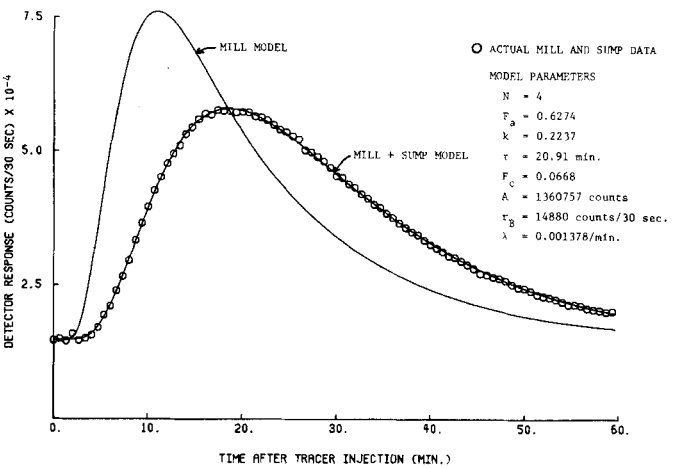

Fig. 15. Actual and fitted detector response data obtained for the 3.81 m × 5.18 m industrial, wet, ball mill at a mill feed rate of 17.7 kg/s.

however, since the finite-stage model introduces the concepts of live vs. dead flow regions, some observations may be made about the transport characteristics of these processes which come directly from the analysis of the RTD data. The ball mills have a larger fraction of live flow region; this is not unexpected, since one would expect that the tumbling of balls and powder would tend to cause a large degree of material dispersion. The classifier RTD parameters indicate, on the other hand, that some material is retained for a relatively long period

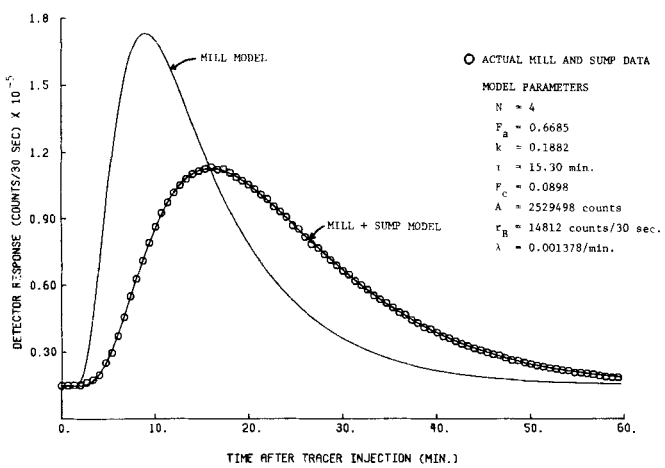

Fig. 16. Actual and fitted detector response data obtained for the 3.81 m × 5.18 m industrial, wet, ball mill at a mill feed rate of 21.4 kg/s.

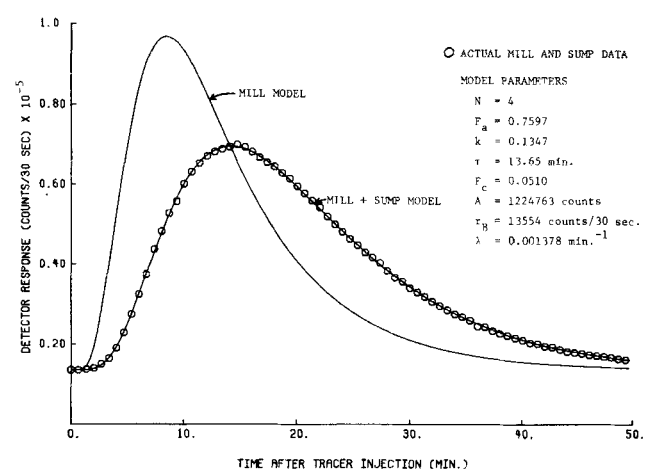

Fig. 17. Actual and fitted detector response data obtained for the 3.81 m × 5.18 m industrial, wet, ball mill at a mill feed rate of 25.2 kg/s.

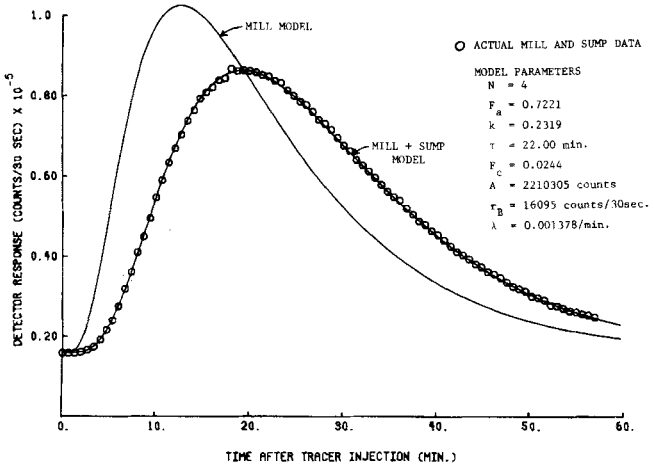

Fig. 18. Actual and fitted detector response data obtained for the 4.57 m × 9.30 m industrial, wet, ball mill at a mill feed rate of 40.4 kg/s.

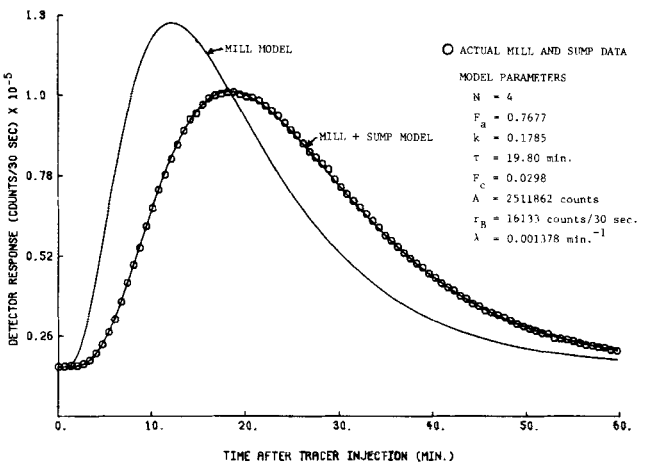

Fig. 19. Actual and fitted detector response data obtained for the 4.57 m × 9.30 m industrial, wet, ball mill at a mill feed rate of 44.1 kg/s.

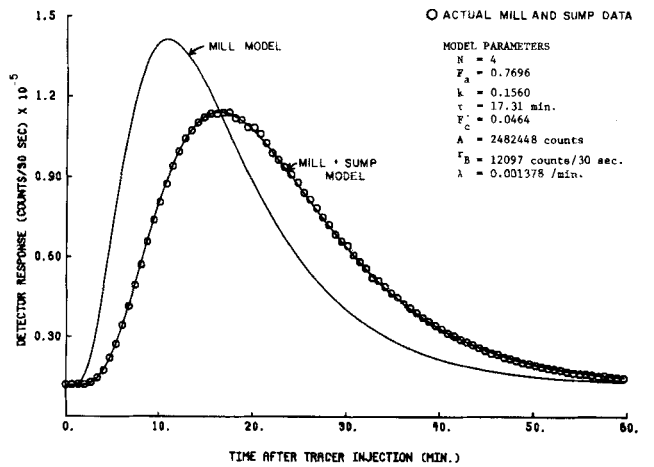

Fig. 20. Actual and fitted detector response data obtained for the 4.57 m × 9.30 m industrial, wet, ball mill at a mill feed rate of 51.7 kg/s.

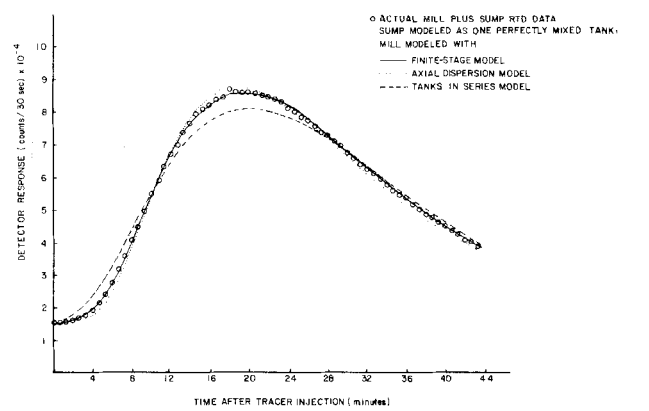

Fig. 21. Comparison of actual and fitted detector response data obtained for the 4.57 m × 9.30 m industrial, wet, ball mill at a mill feed rate of 40.4 kg/s.

of time but undergoes only a small degree of mixing. This result is reasonable, since the spacing between the screw and the classifier shell causes the classification of smaller particles to eventually become a random process (that is, for each rotation of the screw some particles of a given size are retained while others are removed; the net result is an apparent stagnation of some material in the classifier). While it is not possible at this time to characterize the actual microscopic movement of particles through these processes, the finite-stage model allows some physical interpretation of the transport phenomenon. The simpler transport models such as the tanks in series and axial dispersion models do not offer this advantage.

TABLE 2. REDUCED CHI-SQUARED VALUES* OBTAINED FOR MILL PLUS SUMP RTD DATA FITTED TO VARIOUS MILL PLUS SUMP MODELS

Mill size (m)	Feed rate (kg/s)	Reduced chi-squared values for the assumed mill model: Tanks-in-series	Axial dispersion	Finite stage
4.57 × 9.30	40.4	176.18	62.12	1.44
	44.1	209.39	83.57	1.19
	51.7	337.03	166.94	1.68
3.81 × 5.18	17.7	675.18	143.71	2.94
	21.4	2 508.77	725.54	3.68
	25.2	577.92	117.37	1.64

* The variance in the data was taken to be due to radiation counting statistics.

The next consideration is the accuracy of the finite-stage model as compared to simpler models. Figure 21 is a plot of RTD data obtained in a test on the 4.57 m × 9.30 m open-circuit mill at a mill feed rate of 40.4 kg/s. In this figure, the mill and sump data were predicted from Equation (7), where $\phi(t)$ was a mill and sump model. The three curves represent the best fit of a mill and sump model where the finite-stage, tanks-in-series, and axial dispersion models were used to model the mill RTD, and the sump was modeled as a single, perfectly mixed tank whose parameter values are seen in Figure 14. A noninteger number of tanks was allowed in the tanks-in-series model; the axial dispersion model was calculated with the algorithm developed by Rogers (1978). A further comparison was made by computing the reduced chi-squared values* for each of the mill and sump models vs. the actual mill and sump data for the RTD tests on the 3.81 m × 5.81 m and 4.57 m × 9.30 m open-circuit mills. These results are seen in Table 2. It is apparent that the model in which the finite-stage

* The variance in the actual data was taken as that due to radiation counting statistics.

Table 3. Finite-Stage Model Parameters Obtained from the Analysis of RTD Measurements Made on Industrial, Wet, Open-Circuit Ball Mills

Mill size (m)	Feed rate (kg/s)	Finite-stage model parameters N	F_a	F_b	F_c	k	τ (min)
1.83 × 2.74	7.6	4	0.6901	0.3099	0.0	0.1466	8.91
	8.6	4	0.6844	0.3156	0.0	0.1094	8.47
	9.6	4	0.6668	0.3332	0.0	0.1495	7.94
	10.6	4	0.6591	0.3409	0.0	0.1177	7.24
3.81 × 5.18	17.7	4	0.6274	0.3058	0.0668	0.2237	20.91
	21.4	4	0.6685	0.2417	0.0898	0.1882	15.30
	25.2	4	0.7597	0.1893	0.0510	0.1347	13.65
4.57 × 9.30	40.4	4	0.7221	0.2535	0.0244	0.2319	22.00
	44.1	4	0.7677	0.2025	0.0298	0.1785	19.80
	51.7	4	0.7696	0.1840	0.0464	0.1560	17.31
Average values of parameters		4	0.7015	0.2677	0.0308	0.1636	—
Standard deviation of averaged parameters		—	0.0159	0.0188	0.0101	0.0131	—

Table 4. Tanks-in-series and Axial Dispersion Model Parameters Otained From The Analysis of RTD Measurements Made On Industrial, Wet, Open-Circuit, Ball Mills

		Tanks-in-series model		Axial dispersion model
Mill size (m)	Feed rate (kg/s)	Number of tanks, n	τ (min)	Peclet number, Pe*
1.83 × 2.74	7.6	1.73	8.91	1.93
	8.6	1.42	8.47	1.15
	9.6	1.61	7.94	1.62
	10.6	1.35	7.24	0.98
3.81 × 5.18	17.7	1.90	20.91	2.32
	21.4	2.05	15.30	2.66
	25.2	2.35	13.65	3.35
4.57 × 9.20	40.4	2.57	22.00	11.88
	44.1	2.74	19.80	12.21
	51.7	2.79	17.31	14.31

* $Pe = uL/D$, where $u = L/\tau$ = mean axial velocity (m/min), D = dispersion coefficient (m²/min), and L = mill length (m).

concept is used gives a much better prediction of the actual data.

Finally, since this study is part of an overall effort to analyze and simulate open-circuit ball mills, the effect of mill size and operating conditions on the finite-stage model parameters was studied. Table 3 is a compilation of the backcalculated model parameters for all of the ball mill tests described in this study. The pertinent parameters for the tanks-in-series and axial dispersion models are listed for these tests in Table 4. It is seen that the finite-stage model parameters appear to be constant and independent of mill operating conditions, while the parameters of the simpler models are not. This surprising result is probably the most important advantage of utilizing the finite-stage model in ball mill analysis and simulation; the amount of experimental and computational effort can be significantly reduced with the knowledge that the dimensionless RTD is constant.

The advantages of the finite-stage model provided the impetus for developing segregated flow models which incorporate this concept. The authors have derived a steady state segregated flow model for open circuit, continuous grinding and successfully applied it to the analysis and simulation of industrial, open-circuit ball mills (Rogers and Gardner, 1978). Therefore, to aid in the general utilization of the finite-stage concept in segregated flow models, a general, steady state, first-order process model is derived in Appendix C.

ACKNOWLEDGMENT

The authors gratefully acknowledge the help of Mr. Lewis Hash and other personnel of Carolina Silica, Inc., Marston, North Carolina, and of Mr. Charles Peters and other personnel at the W. R. Grace and Co., Bartow, Florida. This work was partially supported by the National Science Foundation under Grant No. ENG75-23257.

NOTATION

$C_{ai}(t)$ = concentration of tracer in the live flow tank of the i^{th} stage at time t after tracer injection
$C_{bi}(t)$ = concentration of tracer in the dead flow tank of the i^{th} stage at time t after tracer injection
C^o = concentration of tracer if uniformly distributed throughout the system
$C_i(t)$ = concentration of tracer leaving the i^{th} stage at time t after tracer injection when the plug flow tanks are omitted
$C_n^*(t)$ = concentration of tracer leaving the final stage at time t after tracer injection
$\delta(t)$ = Dirac delta function in units of reciprocal time
Δt_i = interval of time over which the i^{th} counting rate is obtained
f = fractional flow going through tank number 1 of two perfectly mixed tanks-in-parallel
F_a = fraction of the total system volume in the live flow tanks
F_b = fraction of the total system volume in the dead flow tanks
F_c = fraction of the total system volume in the plug flow tanks
k = fractional cross flow between live and dead flow tanks
q = steady state entry and exit volumetric flow rates to the i^{th} stage in volume per unit time
Q = total amount of tracer injected
r_B = the background counting rate in counts per unit time
r_B^* = estimated background response or detector response in absence of any tracer

t_i = time after tracer injection at which the i^{th} counting rate is obtained
V = total system volume
Y = counting yield in counts per unit time per microcurie per unit volume
$y(t)$ = predicted detector response at the system exit in counts per unit time
y_i = actual counting rate obtained during the i^{th} counting interval

Greek Letters

τ = average residence time of the system
τ_c = time and which detector response appears to rise above r_B*
τ_s = average residence time of a counting sump which is modeled as a single perfectly mixed tank
τ_1 = average residence time of tank number 1 of two perfectly mixed tanks-in-parallel
τ_2 = average residence time of tank number 2 of two perfectly mixed tanks-in-parallel

APPENDIX A: DERIVATION OF THE BASIC MODEL

It is easily shown that the response of a series of n finite stages like that shown in Figure 1 is equivalent to the response of n otherwise identical finite stages without the plug flow tanks followed by one large plug flow tank of size F_cV. Therefore, the derivation will be developed by first deriving the response for n finite stages without the plug flow tanks and then adding on the plug flow response.

A mass balance on the remaining components (tanks a and b) of the i^{th} stage of a system of n series connected stages gives the following sets of differential equations:

$$(F_aV/n)\frac{dC_{ai}(t)}{dt} = qC_{i-1}(t) - qC_{ai}(t) - kqC_{ai}(t) + kqC_{bi}(t) \quad 1 \leq i \leq n \quad (A1)$$

$$(F_bV/n)\frac{dC_{bi}(t)}{dt} = kqC_{ai}(t) - kqC_{bi}(t) \quad 1 \leq i \leq n \quad (A2)$$

Since the plug flow tanks are being omitted from the derivation, one has that

$$C_{ai}(t) = C_i(t) \quad 1 \leq i \leq n \quad (A3)$$

By defining the average residence time τ to be

$$\tau = V/q \quad (A4)$$

and substituting Equations (A3) and (A4) into Equations (A1) and (A2), we get

$$(F_a\tau/n)\frac{dC_i(t)}{dt} = C_{i-1}(t) - (1+k)C_i(t) + kC_{bi}(t) \quad 1 \leq i \leq n \quad (A5)$$

$$(F_b\tau/n)\frac{dC_{bi}(t)}{dt} = kC_i(t) - kC_{bi}(t) \quad 1 \leq i \leq n \quad (A6)$$

For development of the unit impulse response, the pertinent initial conditions are:

$$C_i(0) = 0 \quad 1 \leq i \leq n \quad (A7)$$

and

$$C_o(0) = \delta(t)C^oV/q \quad (A8)$$

Taking the Laplace transforms of Equations (A5) and (A6), we get

$$(F_a\tau/n)s\bar{C}_i(s) = \bar{C}_{i-1}(s) - (1+k)\bar{C}_i(s) + k\bar{C}_{bi}(s) \quad 1 \leq i \leq n \quad (A9)$$

$$(F_b\tau/n)s\bar{C}_{bi}(s) = k\bar{C}_i(s) - k\bar{C}_{bi}(s) \quad 1 \leq i \leq n \quad (A10)$$

Solving Equation (10) for $\bar{C}_{bi}(s)$, we get

$$\bar{C}_{bi}(s) = (nk/F_b\tau)\bar{C}_i(s)/[s + (nk/F_b\tau)] \quad 1 \leq i \leq n \quad (A11)$$

Substitution of $\bar{C}_{bi}(s)$ from Equation (A11) into Equation (A9) and solving for $C_i(s)$, we get

$$\bar{C}_i(s) = C_{i-1}(s)\left(\frac{n}{F_a\tau}\right)\left[\frac{s + nk/F_b\tau}{(s-m_1)(s-m_2)}\right] \quad 1 \leq i \leq n \quad (A12)$$

where

$$\left.\begin{matrix}(+)\, m_1 \\ (-)\, m_2\end{matrix}\right] = -(n/\tau)\left[\frac{F_ak + F_b(1+k)}{2F_aF_b}\right]\left[1 \pm \sqrt{1 - \frac{4kF_aF_b}{[F_ak + F_b(1+k)]^2}}\right] \quad (A13)$$

Solving for the last stage ($i = n$), we get

$$\bar{C}_n(s) = \bar{C}_{n-1}(s)\left(\frac{n}{F_a\tau}\right)\left[\frac{s + nk/F_b\tau}{(s-m_1)(s-m_2)}\right] = \bar{C}_{n-2}(s)\left(\frac{n}{F_a\tau}\right)^2\left[\frac{s + nk/F_b\tau}{(s-m_1)(s-m_2)}\right]^2 = \bar{C}_o(s)\left(\frac{n}{F_a\tau}\right)^n\left[\frac{s + nk/F_b\tau}{(s-m_1)(s-m_2)}\right]^n \quad (A14)$$

Taking the Laplace transform of Equation (A8), we get

$$\bar{C}_o(s) = C^oV/q \quad (A15)$$

Substituting $\bar{C}_o(s)$ from Equation (A5) into Equation (A14), we get

$$\bar{C}_n(s) = (C^oV/q)\left(\frac{n}{F_a\tau}\right)^n\left[\frac{s + nk/F_b\tau}{(s-m_1)(s-m_2)}\right]^n \quad (A16)$$

It can be shown that the inverse transform of Equation (A16) is

$$C_n(t) = (C^oV/q)\left(\frac{n}{F_a\tau}\right)^n \sum_{j=1}^{2}\sum_{l=1}^{n}\frac{\phi_l(m_j)t^{n-l}e^{m_jt}}{(n-l)!(l-1)!} \quad (A17)$$

where

$$\phi_l(m_j) = \left[\frac{m_j + nk/F_b\tau}{m_j - m_i}\right]^n \sum_{r=1}^{l}\frac{(n-1+r)!(-1)^r b_{lr}}{(n-1+1+r)!(m_j + nk/F_b\tau)^{l-1-r}(m_j - m_i)^r} \quad m_j \neq m_i \quad (A18)$$

and the b_{lr} are the binomial coefficients:

$b_{11} = 1$

$b_{21} = 1 \quad b_{22} = 1$

$b_{31} = 1 \quad b_{32} = 2 \quad b_{33} = 1$

$b_{41} = 1 \quad b_{42} = 3 \quad b_{43} = 3 \quad b_{44} = 1$

Now the final solution is obtained by modifying the derived model response for the constant time lag. This is done by

$$C_n^*(t) = C_n(t - F_c\tau)H(t - F_c\tau) \quad (A19)$$

where $H(t)$ is the unit step function such that

$$H(t - F_c\tau) = 0 \quad \text{for} \quad t < F_c\tau$$

$$H(t - F_c\tau) = 1 \quad \text{for} \quad t \geq F_c\tau$$

APPENDIX B: EXTENSIONS OF THE FINITE-STAGE TRANSPORT CONCEPT TO INCLUDE A COUNTING SUMP

The RTD of a process followed by a counting sump is given by

$$\phi_T(t) = \int_o^t \phi(t')\phi_s(t - t')dt' \qquad (B1)$$

The function $\phi(t)$ is taken to be the finite-state transport model, and $\phi_s(t)$ is first assumed to be a single, perfectly mixed tank with average residence time τ_s. In this case, $\phi_s(t)$ is given by

$$\phi_s(t) = \exp(-t/\tau_s)/\tau_s \qquad (B2)$$

and $\phi_T(t)$ is

$$\phi_T(t) = \left(\frac{n}{F_a\bar{\tau}}\right)^n \frac{e^{-t/\tau_s}}{\tau_s} \sum_{r=1}^{2} \sum_{l=1}^{n} \frac{\phi_l(m_r)I_l(m_r)}{(n-l)!(l-1)!} \qquad (B3)$$

where

$$I_l(m_r) = \int_o^t u^{n-l}e^{(m_r+1/\tau_s)u}du \qquad (B4)$$

Equation (B4) is of the form $\int x^m e^{ax}dx$. It can be shown that this integral is given by

$$\int x^m e^{ax}dx = e^{ax} \sum_{k=1}^{m+1} \frac{(-1)^{k+1}x^{m+1-k}m!}{a^k(m+1-k)!} \qquad (B5)$$

Performing the integration of Equation (B4) according to Equation (B5) and inserting the limits, we obtain

$$I_l(m_r) = e^{(m_r+1/\tau_s)t} \sum_{k=1}^{n-l+1} \frac{(-1)^{k+1}(n-l)!t^{n-l+1-k}}{(n-l+1-k)!(m_r+1/\tau_s)^k} + \frac{(-1)^{n-l+1}(n-l)!}{(m_r+1/\tau_s)^{n-l+1}} \qquad (B6)$$

Insertion of Equation (B6) with the appropriate arguments into Equation (B3) completes the derivation.

For the case where $\phi_s(t)$ is taken as two perfectly mixed tanks-in-parallel

$$\phi_s(t) = \frac{f}{\tau_1}e^{-t/\tau_1} + \frac{(1-f)}{\tau_2}e^{-t/\tau_2} \qquad (B7)$$

and $\phi_T(t)$ is given by

$$\phi_T(t) = \left(\frac{n}{F_a\bar{\tau}}\right)^n \sum_{j=1}^{2} a_j \frac{e^{-t/\tau_j}}{\tau_j} \sum_{r=1}^{2} \sum_{l=1}^{n} \frac{\phi_l(m_r)I_{lj}(m_r)}{(n-l)!(l-1)!} \qquad (B8)$$

where

$$a_1 = f$$

$$a_2 = 1 - f$$

and

$$I_{lj}(m_r) = \int_o^t u^{n-l}e^{(m_r+1/\tau_j)u}du \qquad (B9)$$

This integral is identical in form to Equation (B4). Evaluating it according to Equation (B5) and inserting the limits and then substituting the appropriate arguments, we complete the derivation of the closed form expression for Equation (B8).

APPENDIX C: INCORPORATION OF THE MODEL INTO CONTINUOUS FIRST-ORDER PROCESS MODELS

In all continuous processes, both the process phenomenon and the material transport and dispersion phenomena are important. In many cases, it is possible to develop analytical models for both of these phenomena separately, which result in analytical models for the entire process. In particular, the segregated flow model concept can often be used for accomplishing this. This concept essentially consists of assuming that the steady state product variable of interest can be obtained by averaging the batch model variable of interest according to the residence time distribution. The present finite-stage transport model has a major advantage in that it can be combined with common first-order process phenomena to give models with analytical solutions. This is also true of the tanks-in-series transport model. To aid in the utilization of the finite-stage transport concept, an analytical solution is given here for the case when it is incorporated with a general steady state continuous first-order process.

A general first-order reaction is represented here by species A reacting to produce species B in a one-to-one ratio. This idealized batch reaction would occur if, in a constant volume batch reactor, a fixed amount of species A is suddenly introduced to obtain a uniform concentration and it reacts uniformly throughout the reactor to produce species B. The batch reaction equation for this system is modeled as (Levenspiel, 1962).

$$C_A(t) = C_A(0)e^{-kt} = [C_A(t)]_{\text{BATCH}} \qquad (C1)$$

where $C_A(t)$ is the concentration of A in the reactor as a function of time, and k is the reaction rate constant. Now, if the same reactor were to be used in the continuous open-circuit mode, a steady state model for the concentration of A in the product stream could be determined by the use of the segregated flow concept. This concept is mathematically stated as

$$C_{AP} = \int_o^\infty [C_A(t)]_{\text{BATCH}}\phi(t)dt \qquad (C2)$$

where C_{AP} is the steady state concentration of A in the product. For the first-order process

$$C_{AP} = \int_o^\infty C_{AF}e^{-kt}\phi(t)dt \qquad (C3)$$

where C_{AF} is the concentration of A in the feed stream and is equivalent to $C_A(0)$ and $\phi(t)$ is the normalized RTD of A. If $\phi(t)$ is taken to be the finite-stage transport model in Equation (C3), the expression for C_{AP} becomes

$$C_{AP} = C_{AF}\left(\frac{n}{F_a\bar{\tau}}\right)^n \sum_{r=1}^{2} \sum_{l=1}^{n} \frac{\phi_l(m_r)}{(n-l)!(l-1)!} \int_o^\infty t^{n-l}e^{(m_r-k)t}dt \qquad (C4)$$

The integral in Equation (A10) is of the form $\int_o^\infty x^m e^{ax}dx$.

It can be shown that this integral is given by

$$\int_o^\infty x^m e^{ax}dx = \frac{(-1)^{m+1}m!}{a^{m+1}} \qquad (C5)$$

Performing the integration in Equation (A10), we obtain

$$C_{AP} = C_{AF}\left(\frac{n}{F_a}\right)^n \sum_{r=1}^{2} \sum_{l=1}^{n} \frac{\phi_l(m_r)(-1)^{n-l+1}}{(l-1)!(m_r-k)^{n-l+1}} \qquad (C6)$$

LITERATURE CITED

Adler, R. J., and R. B. Hovorka, "A Finite-Stage Model for Highly Asymmetric Residence Time Distributions," *Digest of Technical Papers*, 34, Second Joint Auto. Control Conf. (1961).

Bevington, P. R., Data Reduction and Error Analysis for the Physical Sciences, McGraw-Hill, New York (1969).

Gardner, R. P., and R. L. Ely, Jr., *Radioisotope Measurement Applications in Engineering*, Reinhold, New York (1967).

Gardner, R. P., R. S. Rogers, and K. Verghese, "Short-Lived Radioactive Tracer Methods for the Dynamic Analysis and Control of Continuous Comminution Processes by the Mechanistic Approach," *Intern. J. Appl. Rad. Isotopes*, **28**, No. 10/11, 861 (1977).

Himmelblau, D. M., and K. B. Bischoff, *Process Analysis and Simulation*, Wiley, New York (1968).

Kelsall, D. F., and K. J. Reid, "The Derivation of a Mathematical Model for Breakage in a Small, Continuous, Wet, Ball Mill, in Application of Mathematical Models in Chemical Engineering Research, Design and Production," *Inst. Chem. Engrs. Symposium Ser. No. 4*, 14 (1965).
Levenspiel, O., *Chemical Reaction Engineering*, Wiley, New York (1962).
Reid, K. J., "A Solution to the Batch Grinding Equation," *Chem. Eng. Sci.*, **20**, No. 11, 952 (1965).
Rogers, R. S. C., "A Simple Algorithm for Calculating Residence Time Distribution From the Axial Dispersion Flow Concept," to be submitted to *Powder Technol.* (1979).
———, and R. P. Gardner, "Application of a Finite-Stage Transport Concept to the Analysis and Simulation of Open-Circuit, Industrial Ball Mills by the Mechanistic Approach," to be submitted to *AIChe J.* (1979).

Manuscript received March 17, 1978; revision received August 25, and accepted November 22, 1978.

Annular Two-Phase Flow of Gases and Non-Newtonian Liquids

FRED G. EISENBERG
and
CHARLES B. WEINBERGER
Department of Chemical Engineering
Drexel University
Philadelphia, Pennsylvania 19104

Two-phase, annular flow of gases and non-Newtonian liquids through horizontal pipes is modeled, and a prediction method for pressure drop and gas volume fraction is proposed. The prediction method consists of a modification, based upon shear rate dependence of the apparent viscosity of the liquid phase, of Lockhart-Martinelli correlations for Newtonian liquids. The model applies to the case of laminar flow of the annular liquid film. Experimental data, obtained with several aqueous polymer solutions and air, agree closely with predicted values of pressure drop and void fraction.

SCOPE

The objective of this work is to develop techniques which enable prediction of pressure drop and gas volume fraction for two-phase, concurrent flow of gases and non-Newtonian liquids for the annular flow regime. This predictive capability is relevant to such processes as continuous polymerization reactors, direct contact drying of non-Newtonian liquid foods, etc.

Previous attempts to model two-phase, annular flow of gases and non-Newtonian liquids have included the assumption of a smooth gas-liquid interface. Partly as a result of this assumption, rather large discrepancies between predicted and experimental values of pressure drop and gas volume fraction have been observed. By basing a prediction scheme for non-Newtonian liquids on existing empirical correlations for Newtonian liquids, this assumption can be largely avoided.

The proposed prediction scheme accounts for the shear rate thinning behavior of pseudoplastic liquids. Since the average shear rate in the liquid phase is greater in the case of two-phase flow than in single-phase flow at the same flow rate, the average viscosity is taken into account quantitatively, using a power law fluid model. Effects directly attributable to the elasticity of the liquid are beyond the scope of this work.

Experimental data are presented for several types of aqueous polymer solutions at various concentration levels; these include three types in this work and three types used by previous investigators.

CONCLUSIONS AND SIGNIFICANCE

Based upon a comparison of predicted and measured pressure drops for annular, two-phase flow of gases and pseudoplastic fluids, the prediction scheme proposed here is quite successful. When the viscosity correction is not applied, the Lockhart-Martinelli correlation yields predicted values of pressure gradient which are approximately three times the measured values; however, when the correction is applied, the average discrepancy using the proposed prediction scheme is roughly 5% for all the solutions except Polyox. For the Polyox solutions, the predicted pressure drop is 10 to 40% less than the measured value; such disagreement appears to be attributable to the inadequacy of a simple power law fluid model to describe the rheological response of this type of solution in such two-phase flows.

Similarly, predicted values for the gas volume fraction agree, within about 10%, with measured values. For the results obtained in this laboratory, the measured volume fractions are slightly lower than predicted, whereas for the data obtained by previous investigators, the measured values are slightly higher.

Correspondence concerning this paper should be addressed to C. B. Weinberger. F. G. Eisenberg is with the Air Products Company, Allentown, Pennsylvania.